

Diurnal cycles in Arctic surface radiative fluxes in a blended satellite-climate reanalysis data set

Xuanji Wang^{*}, Jeffrey R. Key[†], Chuck Fowler⁺, James Maslanik[&]

^{*}*Cooperative Institute for Meteorological Satellite Studies, University of Wisconsin-Madison
Madison, Wisconsin 53706, USA*

xuanjiw@ssec.wisc.edu

[†]*Center for Satellite Applications and Research, NOAA/NESDIS, Madison, Wisconsin 53706,
USA*

jkey@ssec.wisc.edu

⁺*Colorado Center for Astrodynamics Research, University of Colorado, Boulder, Colorado,
USA*

Charles.Fowler@colorado.edu

[&] *Cooperative Institute for Research in the Environmental Sciences, University of Colorado
Boulder, Colorado, USA*

james.maslanik@colorado.edu

Abstract. Surface radiative fluxes and their diurnal cycles are very important components in the surface energy budget of the Arctic, and also critical forcing variables for land surface models. An approach has been developed to derive diurnal cycles of the surface radiative fluxes for the Arctic from 6-hourly accumulated surface downward shortwave and longwave radiative fluxes in the European Center for Medium Range Weather Forecasts (ECMWF) 40-year reanalysis (ERA-40) products by “correcting” interpolated hourly values with twice-daily satellite-derived radiative fluxes. Ground-based measurements of the surface radiative fluxes at an Arctic meteorological station are used to validate the approach. Results show that the blended satellite-model products are in good agreement with the ground-based measurements. Based on this blended product, diurnal cycles of surface radiative fluxes are examined over time and space. It clearly shows that satellite-retrieved products in high spatial and temporal resolutions are more realistic and accurate, and can be used to adjust or “correct” the reanalysis products, especially for the polar region where there exist few ground based measurements for diurnal cycle studies.

Keywords: Arctic climate, APP-x, ECMWF, surface radiative flux, reanalysis data.

1 INTRODUCTION

Numerical weather and climate model studies have demonstrated that the Arctic is one of the most sensitive regions on Earth to global climate change [1-4]. Recent Arctic climate change studies with observational data from ground-based measurements, field experiments, and satellite retrieved products also show that the Arctic is indeed experiencing greater climate change than ever before [5-18]. Changes in the Arctic climate are associated with the changes in the hydrological cycle, cloud and aerosol variations, evolving ecosystems, and dynamical perturbations, which eventually feed back to the global climate. Diurnal cycles of the surface radiative fluxes are important components of the surface energy budget, and are therefore important forcing variables to land surface models. Unfortunately, the Arctic is a data sparse region with very few in-situ observations, most of them being in the coastal areas. Field experiments and buoy measurements provide only short time period data for some specific locations.

An alternative approach to gaining a better understanding of the Arctic weather and climate, particularly diurnal cycles, is to use numerical climate model analyses combined with satellite data. The assumption is that satellites provide more accurate estimates of some geophysical variables and do so with high resolution spatial coverage. However, satellites do not provide the temporal sampling (hourly or 6-hourly) that models do. While some satellite data and derived products, such as radiance data, cloud amount, cloud motion wind, ozone amount, and atmospheric profile (refer to <http://www.ecmwf.int/research/era/Observations/>), have been assimilated in reanalysis products from the National Centers for Environmental Prediction (NCEP)/National Center for Atmospheric Research (NCAR) and the European Centre for Medium Range Weather Forecasts (ECMWF), new satellite products can be used to adjust or “correct” the reanalysis products, especially for the polar regions

In this study, an approach is developed to derive hourly downwelling shortwave and longwave fluxes from the 6-hourly accumulated fluxes in the ECMWF Reanalysis ERA-40 product. Ground-based measurements from one Arctic station are used to validate derived diurnal cycles of surface radiative fluxes, and are compared to the Advanced Very High Resolution Radiometer (AVHRR) Polar Pathfinder extended (APP-x) products. A correction algorithm is developed to blend or “correct” ERA-40 derived diurnal cycle data with APP-x data at specific times.

2 DATA

The ECMWF 40-year reanalysis (ERA-40) currently covers the period September 1957 to August 2002, overlapping the earlier ECMWF 15-year reanalysis called ERA-15 over 1979-1993 [19]. ERA-40 basic surface and pressure level analyses interpolated to a $2.5^\circ \times 2.5^\circ$ regular latitude/longitude grid were used in this study. ERA-40 reanalysis fields are analyses for 00:00, 06:00, 12:00, and 18:00 UTC each day, including many variables, but surface downwelling shortwave and longwave fluxes are accumulations over 6-hour intervals, making it impossible to directly determine diurnal cycles. A method to convert 6-hourly accumulation into hourly radiative fluxes is presented in the next section.

The AVHRR Polar Pathfinder (APP) data set consists of twice-daily composites at a 5×5 km² pixel size over the period 1982-2004. The consistency of the retrieved products from different NOAA polar orbital satellites over the period 1982 to 2004 was investigated by Wang and Key (2003) [5] and found having no observable bias. The APP data set was extended (hereinafter “APP-x”) to include the retrievals of cloud cover, cloud optical depth, cloud particle phase and size, cloud top temperature and pressure, cloud type, surface skin temperature, surface broadband albedo, and radiative fluxes as well as cloud radiative effects (“cloud forcing”). For computational considerations the original 5 km APP data were sub-sampled to 25 km by picking up the central pixel in a 5×5 pixel box. Retrievals were done with the Cloud and Surface Parameter Retrieval (CASPR) system [20,21], which was specially designed for polar AVHRR daytime and nighttime product retrievals. All parameters are retrieved at all times, day or night. Radiative fluxes are calculated in the CASPR using FluxNet [22], which is a neural network version of radiation transfer model called Streamer [23]. The atmospheric profiles of temperature and humidity from the NCEP/NCAR reanalysis data set provided by NOAA-CIRES Climate Diagnostics Center, Boulder, Colorado, USA, and the ISCCP D2 ozone data [24] provided by NASA Langley Research Center were also used in CASPR retrieval process. The daily APP-x composites are centered on the local solar time of 14:00 (high sun, but could be nighttime for some Arctic regions in winter) and 04:00 (low sun, but could be daytime for some Arctic regions in summer).

The APP-x products have been validated with the data collected during the Surface Heat Balance of the Arctic Ocean (SHEBA) field experiment in the western Arctic [25,26], and with the data from two Antarctic meteorological stations: South Pole and Neumayer [27]. The APP-x products were primarily compared with SHEBA ship measurements for the purpose of

error estimation by averaging APP-x 5 x 5 pixel boxes (25 x 25 km²) centered on the SHEBA ship site [6,7].

3 DERIVING DIURNAL CYCLES FROM ERA-40

The ERA-40 downwelling shortwave and longwave fluxes are accumulations over 6-hour intervals, and therefore must be converted to hourly values. For this conversion, relatively simple parameterizations are used.

3.1 Surface downwelling solar radiative flux

There exist a variety of methods for the estimation of clear- and cloudy-sky solar and terrestrial radiation fluxes at the surface for the Arctic. Based on a comparison by Key et al. (1996) [28], a simple formula by Bennett (1982) [29] was selected for the estimation of clear-sky solar radiative flux at the surface:

$$SW_{\downarrow\text{clr}} = 0.72 S_0 \cos Z, \quad (1)$$

where S_0 is the solar constant, Z is the solar zenith angle, and $SW_{\downarrow\text{clr}}$ is surface downwelling solar radiative flux under clear-sky conditions. For the estimation of the solar radiative flux under all-sky conditions in the Arctic, the Jacobs (1978) [30] formula is employed:

$$SW_{\downarrow\text{all}} = SW_{\downarrow\text{clr}}(1 - 0.33c), \quad (2)$$

where c is the cloud cover at the time of flux calculation to be interpolated from 6-hourly ERA-40 data and corrected by the APP-x data (discussed later), and $SW_{\downarrow\text{all}}$ is surface downwelling solar radiative flux under all-sky conditions. Thus, for each ERA-40 grid, the all-sky solar radiative flux can be calculated by using the above formulas, with local solar zenith angles calculated from the local time and latitude/longitude, and cloud cover obtained by interpolating 4 times a day to 24 times a day and assuming that cloudiness changes within 6-hour interval are linear in the ERA-40 data.

ERA-40 flux data are given as accumulations over each 6-hour interval, so it is necessary to convert to instantaneous fluxes for each hour. It is assumed that the accumulation of theoretically calculated fluxes over the 6-hour interval by equations (1) and (2) should be proportional to the actual ERA-40 accumulation over the same time period, and the following relationship should be valid for both:

$$SW_{\downarrow\text{cal}} / \text{TOTAL}(SW_{\downarrow\text{cal}})_{6\text{hrs}} = SW_{\downarrow\text{era}} / (\text{ERA-40 6-hour accumulation}), \quad (3)$$

where $SW_{\downarrow\text{cal}}$ and $SW_{\downarrow\text{era}}$ are the surface solar radiative fluxes at a specific time within the accumulation time period. The actual solar flux $SW_{\downarrow\text{era}}$ at a specific time can then be derived from equation (3).

3.2 Surface downwelling longwave radiative flux

A parameterization of the clear-sky longwave radiative flux by Idso and Jackson (1969) [31] was selected:

$$LW_{\downarrow\text{clr}} = \sigma T^4 [1 - 0.261 \exp\{-7.77 \times 10^{-4} (273 - T)^2\}], \quad (4)$$

where $LW_{\downarrow\text{clr}}$ is the surface downwelling longwave radiative flux under clear-sky conditions, σ is the Stefan-Boltzmann constant, and T is the near-surface air temperature. The all-sky surface downwelling longwave radiative flux can be calculated by using the Jacobs (1978)

[30] formula:

$$LW\downarrow_{all} = LW\downarrow_{clr} (1 + 0.26c), \quad (5)$$

where $LW\downarrow_{all}$ is the surface all-sky downwelling longwave radiative flux. Thus, for each ERA-40 grid, the all-sky longwave radiative flux can be calculated by using the above formula (5) since the near-surface air temperatures and cloud cover can be obtained by interpolating the 6-hourly data to hourly values assuming that the changes in cloud cover and air temperature within 6-hour interval are linear.

As with the downwelling solar flux, the ERA-40 surface downwelling longwave flux data are also given as an accumulation over the 6-hour interval, so it is necessary to convert it to a flux at a specific time. It is assumed that the accumulation of theoretically calculated fluxes over the 6-hour interval in equations (4) and (5) should be proportional to the actual ERA-40 accumulation over the same time period, and the following relationship should hold, that is:

$$LW\downarrow_{cal} / \text{TOTAL}(LW\downarrow_{cal})_{6hrs} = LW\downarrow_{era} / (\text{ERA-40 6-hour accumulation}), \quad (6)$$

where $LW\downarrow_{cal}$ and $LW\downarrow_{era}$ are the surface downwelling longwave radiative fluxes at a specific time within the accumulation time period, i.e., a 6-hour interval, from above calculation and ERA-40.

3.3 Other parameters

In order to estimate the diurnal cycles of the downwelling shortwave and longwave fluxes and to blend them with satellite observations, we need hourly values of cloud cover, near-surface air temperature and dew-point temperature, solar zenith angle, surface broadband albedo, and cloud visible optical depth. Hourly values were estimated by using simple linear interpolation between the 4-times per day ERA-40 data or the twice daily APP-x product. The variables that are derived from ERA-40 are total cloud cover, 2-meter air temperature, 2-meter dew-point air temperature, solar zenith angle, while the APP-x provides total cloud cover, cloud visible optical depth, and surface broadband albedo.

4 COMPARISON BETWEEN ERA-40, APP-X, AND GROUND MEASUREMENTS

To intercompare ERA-40, APP-x, and ground-based measurements of surface radiative fluxes, meteorological station measurements from Kougark Site 2 at 65°25.70'N, 164°38.61'W in Alaska were used. The station measurements were taken from 10-meter meteorological towers during the Arctic Transitions in the Land-Atmosphere System (ATLAS) project [32]. The ground-based measurements of the surface radiative fluxes are available on an hourly time scale since 1999.

Figure 1 shows the comparisons between these three data sets for the surface downwelling shortwave radiative fluxes in September, 1999. Cloudiness estimates from APP-x and ERA-40 are also shown in the figure. The ERA-40 reanalysis data for Kougark is the result of bilinear interpolation, and the APP-x data for Kougark is the result of averaging a box of 5 x 5 pixels, i.e., an area of 125 km x 125 km, centered on the Kougark site. The ground-based measurements at Kougark are only available for the months of July, August, September, and October with most measurements in September. Overall, the APP-x is better than the ERA-40 in comparison to the ground-based measurements. For a total of 133 available measurements in 1999, the mean of the station measurements is 155.84 Wm^{-2} ; the mean from APP-x is 154.07 Wm^{-2} , and the mean from ERA-40 is 159.31 Wm^{-2} . APP-x and ERA-40 both well correlated with the surface measurements. Figure 2 shows the same comparisons as Figure 1, but for the surface downwelling longwave radiative fluxes. The ground-based mean is 297.18

Wm^{-2} . The ERA-40 systematically overestimates the longwave fluxes with the mean of 313.11 Wm^{-2} , while the APP-x has the mean of 302.56 Wm^{-2} . Overall, the APP-x provides better estimates of the surface downwelling shortwave and longwave radiative fluxes than ERA-40 in comparison to the ground-based measurements, indicating the potential to improve diurnal cycles of these parameters by “correcting” the reanalysis values at times when satellite data are available.

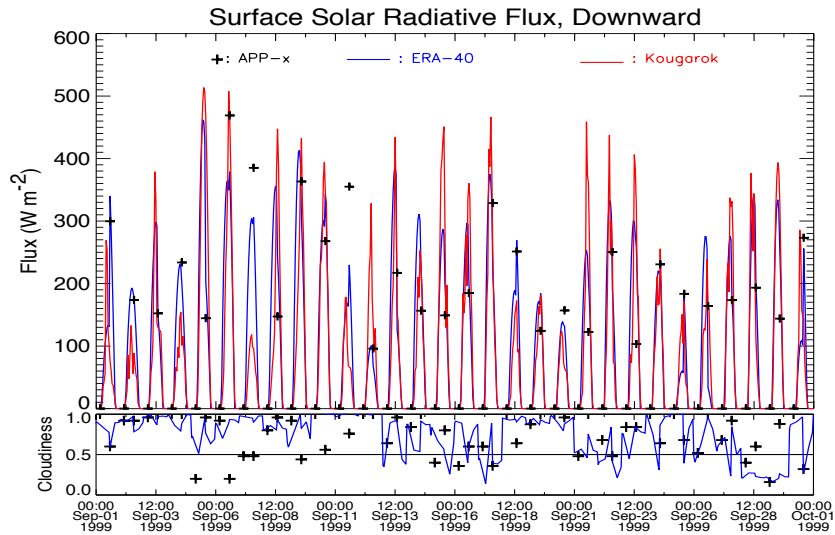


Fig. 1. Comparison of the surface downwelling shortwave radiative fluxes between ERA-40, APP-x, and Kougatok for September, 1999. Red curve stands for the ground-based measurements at Kougatok site, blue curve represents ERA-40, and black crosses denote APP-x. Cloudiness information from ERA-40 and APP-x is also plotted in the bottom panel.

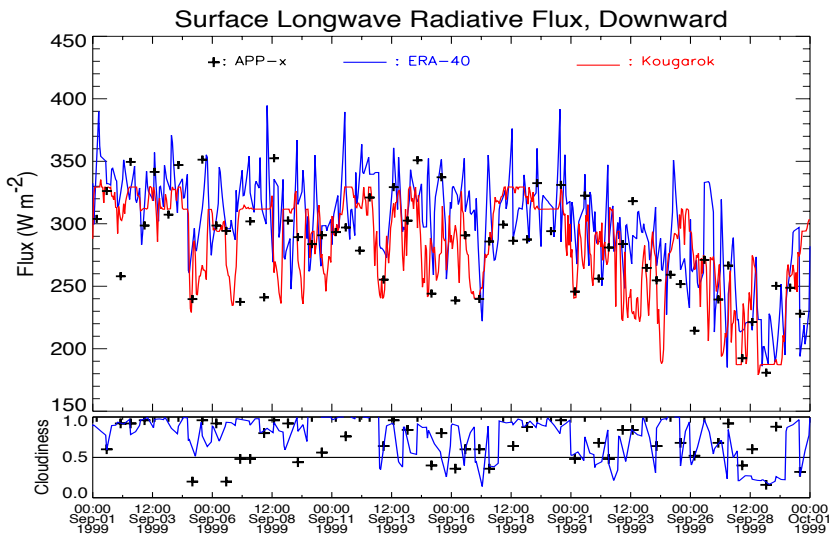


Fig. 2. Same as Figure 1, but for the comparison of the surface downwelling longwave radiative fluxes.

5 CORRECTION ALGORITHM FOR THE BIASES BETWEEN ERA-40 AND APP-X

To blend the satellite data and the model analysis, the systematic bias between two data sets needs to be removed. Based on the comparisons in section 4, the APP-x data set appears to be closer to the ground-based measurements than the modeling analysis. It is therefore reasonable to adjust the ERA-40 diurnal cycle values based on the differences, or biases, between those two data sets. A bias correction can be accomplished by developing bias regression equations, polynomial in form and being based on the differences between the two data sets. Bias regression equations for all grid points have the same form but different coefficients.

For the surface downwelling shortwave radiative flux (hereafter “SSRD”), the bias regression equation takes the form:

$$\begin{aligned} (S_{bias}/(SSRD+I)) = & C_0 + C_1(a+I) + C_2(c+I) + C_3(d+2) + C_4(\mu+I) + C_5(a+I)(c+I) + \\ & C_6(a+I)(d+I) + C_7(a+I)(\mu+I) + C_8(c+I)(d+I) + C_9(c+I)(\mu+I) + \\ & C_{10}(d+I)(\mu+I) + C_{11}(a+I)(c+I)(d+I) + C_{12}(a+I)(c+I)(\mu+I) + \\ & C_{13}(a+I)(d+I)(\mu+I) + C_{14}(c+I)(d+I)(\mu+I) + \\ & C_{15}(a+I)(c+I)(d+I)(\mu+I) \end{aligned} \quad (7)$$

where S_{bias} is ERA-40 minus APP-x, $SSRD$ is ERA-40 surface downwelling shortwave radiative flux, a is the surface broadband albedo from APP-x, c is ERA-40 cloud cover, d is the difference in cloud cover between ERA-40 and APP-x, and μ is the cosine of solar zenith angle. C_{0-15} are regression coefficients (different for each grid point).

The method is similar for the surface downwelling longwave radiative flux (hereafter “STRD”):

$$\begin{aligned} (T_{bias}/(STRD+I)) = & C_0 + C_1(a+I) + C_2(c+I) + C_3(t+2) + C_4(e+I) + C_5(a+I)(c+I) + \\ & C_6(a+I)(t+I) + C_7(a+I)(e+I) + C_8(c+I)(t+I) + C_9(c+I)(e+I) + \\ & C_{10}(t+I)(e+I) + C_{11}(a+I)(c+I)(t+I) + C_{12}(a+I)(c+I)(e+I) + \\ & C_{13}(a+I)(t+I)(e+I) + C_{14}(c+I)(t+I)(e+I) + \\ & C_{15}(a+I)(c+I)(t+I)(e+I) \end{aligned} \quad (8)$$

where T_{bias} is ERA-40 minus APP-x, $STRD$ is ERA-40 surface downwelling longwave radiative flux, a is ERA-40 cloud cover, c is the cloud cover difference between ERA-40 and APP-x, t is blackbody irradiance calculated from the ERA-40 2-meter air temperature with the Stefan-Boltzmann law, i.e., $t = \sigma T_2^4$, e is the difference in blackbody irradiance between the 2-meter air temperature T_2 and 2-meter dew-point temperature T_{d2} , i.e., $e = \sigma T_2^4 - \sigma T_{d2}^4$, and C_{0-15} are the regression coefficients (different for different grid point).

To test the significance of the bias regression equations and validate the method, an independent statistical test was performed. Two time series of the bias data set, one for the creation of the regression equation coefficients (odd numbered years) and the other for statistical testing (even numbered years), were used. Thirty-one locations were chosen for the test by comparing the bias mean and standard deviation before and after the bias corrections. Figure 3 shows an example of the surface downwelling shortwave fluxes at one location (latitude: 70°N, longitude: 180°E). The overall bias and standard deviation for the differences between ERA-40 and APP-x are reduced to 2.36 Wm⁻² from -57.36 Wm⁻² and to 23.95 Wm⁻² from 44.29 Wm⁻² after applying the bias correction algorithms for the downwelling shortwave and longwave fluxes, respectively. Figure 4 shows for the surface downwelling longwave radiative fluxes at the same location. The overall bias and standard deviation are reduced to 1.46 Wm⁻² from 7.60 Wm⁻² and 9.50 Wm⁻² from 14.31 Wm⁻², respectively. This demonstrates the validity and effectiveness of the bias correction algorithms for “correcting” the ERA-40

data set.

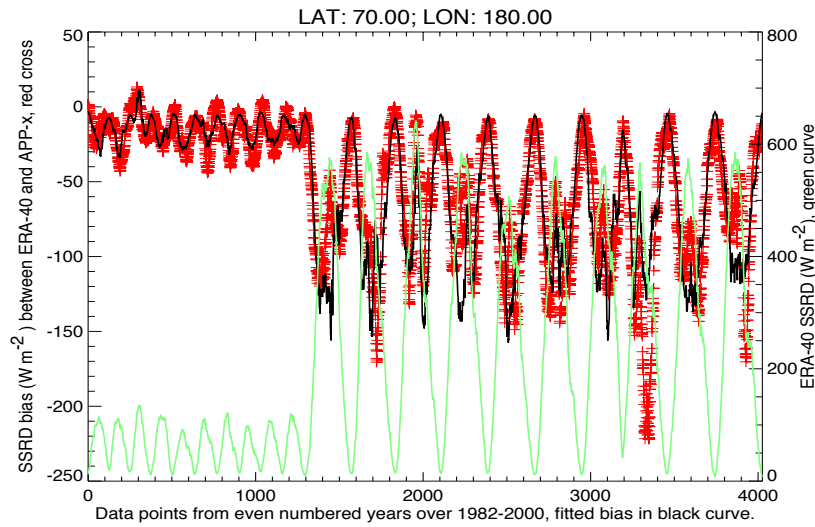


Fig. 3. Real SSRD biases (red crosses) and fitted SSRD biases (black curve) between ERA-40 and APP-x, and the absolute SSRD values (green curve) from ERA-40 over 1982-2000 with even numbered year data being as an independent statistics test data set at the location of the site (70°N, 180°E).

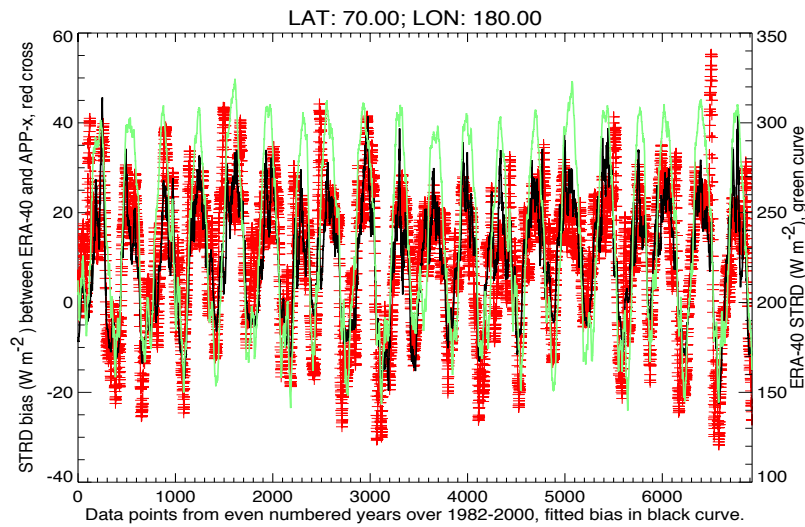


Fig. 4. Same as Figure 3, but for the STRD biases and STRD values from ERA-40.

Figures 5 and 6 show the biases between ERA-40 and the ground-based measurements at Kougarkok before and after applying the correction algorithms. The mean and standard deviation of the differences are given in Table 1 along with the improvement in percent that is defined as the quotient of difference between uncorrected value and corrected value divided by uncorrected value. Both the mean difference and the variability of the differences are reduced considerably. These results clearly show that the bias correction and blending of the satellite and reanalysis data sets result in an improved product.

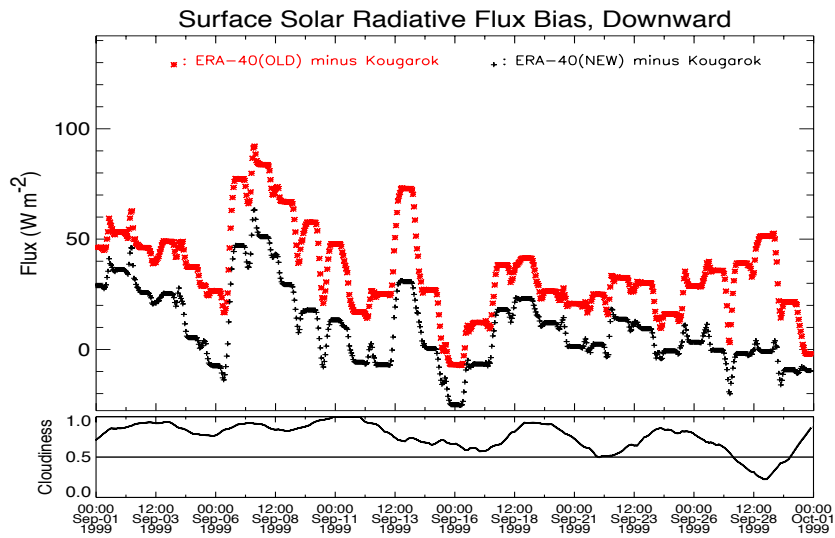


Fig. 5. SSRD biases between ERA-40 and Kougarak ground-based measurements before correction (red stars) and after correction (black crosses) with the APP-x data for September, 1999. Cloudiness from ERA-40 is also plotted in the bottom panel.

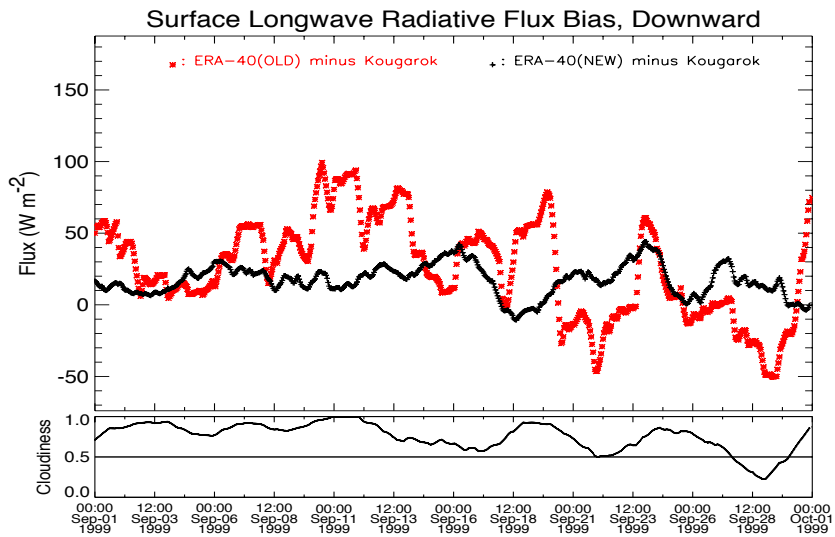


Fig. 6. Same as Figure, but for STRD biases.

Table 1. Bias between ERA-40 and Kougarok Surface Measurements for the Diurnal Cycles of Surface Downwelling Radiative Fluxes in 1999.

Variable Name	Statistics	Uncorrected (W m ⁻²)	Corrected(W m ⁻²)	Improvement (%)
SSRD	Bias	40.11	9.23	77%
	Standard deviation	59.51	44.82	25%
STRD	Bias	35.28	22.38	37%
	Standard Deviation	84.12	31.96	62%

The standard deviation σ of the SSRD is improved about 25% which is less than the SSRD bias improvement (77%), the possible reasons include large variability of the SSRD as seen in Figure 5 due to the changing illumination geometry over time, the model grid cell estimate versus ground-based point measurement, and the inconsistent cloud cover estimates from the two data sets that affect the SSRD estimate significantly, while the relatively bigger improvement on the SSRD bias could also be the result of the cancellation of positive and negative biases taken into the average. The bigger improvement of the STRD standard deviation (62%) than the STRD bias improvement (37%) could be the result of less variability of the STRD over time as seen in Figure 6, making it easier to be regressed than the SSRD, and the different cloud cover estimates from the two data sets because of the different spatial resolution and temporal difference could also make the STRD bias bigger since the STRD values are much more sensitive to cloud cover than to any other factors. The uncertainties in other factors such as surface 2-meter air temperature and dew-point temperature could also add the errors to the estimates of the STRD values. The further investigation on the error sources need to be done in the future study.

6 DERIVED DIURNAL CYCLE DATA SET

Though there has been some research on the use of satellite data for studying diurnal cycles [33,34], diurnal cycles in the polar regions have received little, if any, attention. This is in part due to the difficulty in estimating cloud and surface properties in such extreme meteorological conditions. While problems still remain, new products such as APP-x provide estimates of the surface and cloud properties with accuracies sufficient for many climate studies. Reanalysis products, such as ERA-40, provide complementary information. We now examine diurnal cycles over the Arctic in the blended APP-x/ERA-40 data product, which we call the APP-x Derived Diurnal Cycle (hereinafter “APP-x DDC”) data set.

Figure 7 is an example of the diurnal cycles of the surface downwelling shortwave and longwave radiative fluxes at Kougarok site on January 15, April 15, July 15, and October 15 in 1999 derived from APP-x DDC on an Equal-Area Scalable Earth (EASE) grid with the spatial resolution of 2.5 by 2.5 degrees. Bilinear interpolation was employed to estimate the diurnal cycle data at Kougarok site in local solar time. The cloudiness, which was also derived from our diurnal cycle data set, is also plotted. As expected, the maximum downwelling shortwave flux occurs at local noon, while the variability of the downwelling longwave fluxes over a day resembles more or less the diurnal cycle of cloudiness, but not always true because of prevalent temperature inversion in the Arctic. Of course, the maximum shortwave flux does not always occur at noon because cloud cover varies throughout the day.

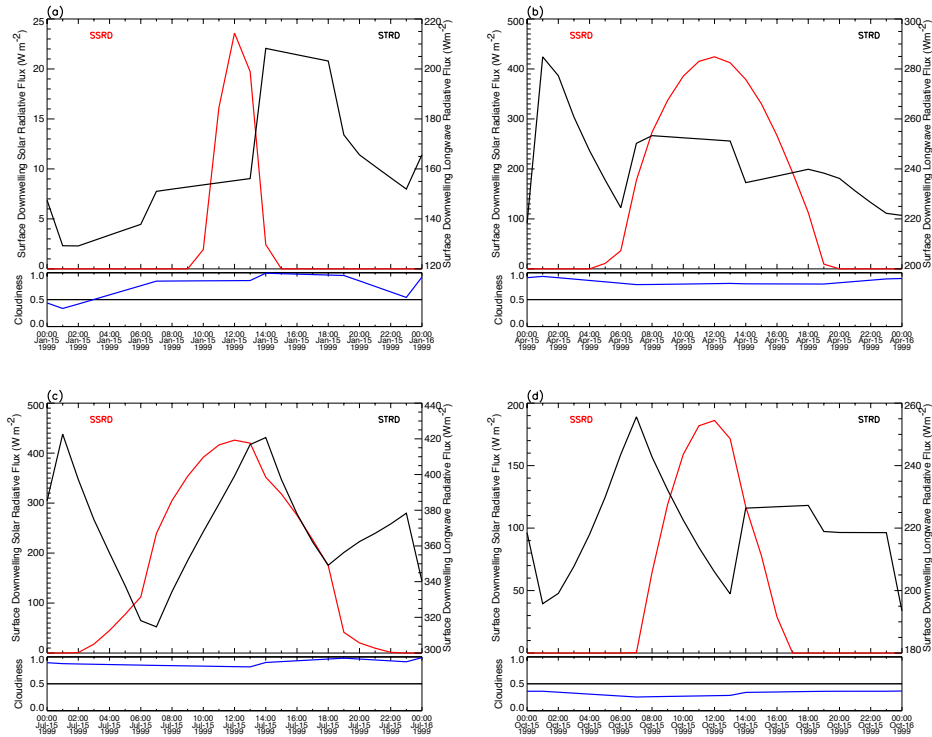
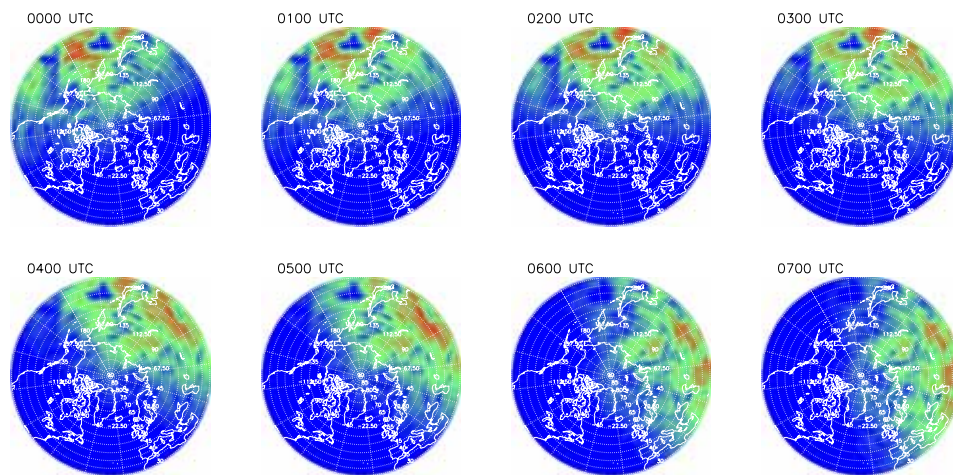


Fig. 7. Diurnal cycles of SSRD (red curve) and STRD (black curve) from APP-x DDC dataset for January 15 (a), April 15 (b), July 15 (c), and October 15 (d) in 1999. The blue curve at the bottom of each plot represents cloudiness from the ERA-40 dataset.

With the APP-x DDC data set, it is also possible to examine the spatial distributions of the diurnal cycles. Figure 8 shows hourly snapshots of the surface shortwave fluxes for the Northern Hemisphere region north of 30°N on July 3, 1999. Figures 9 and 10 show the surface longwave fluxes and cloudiness, respectively.



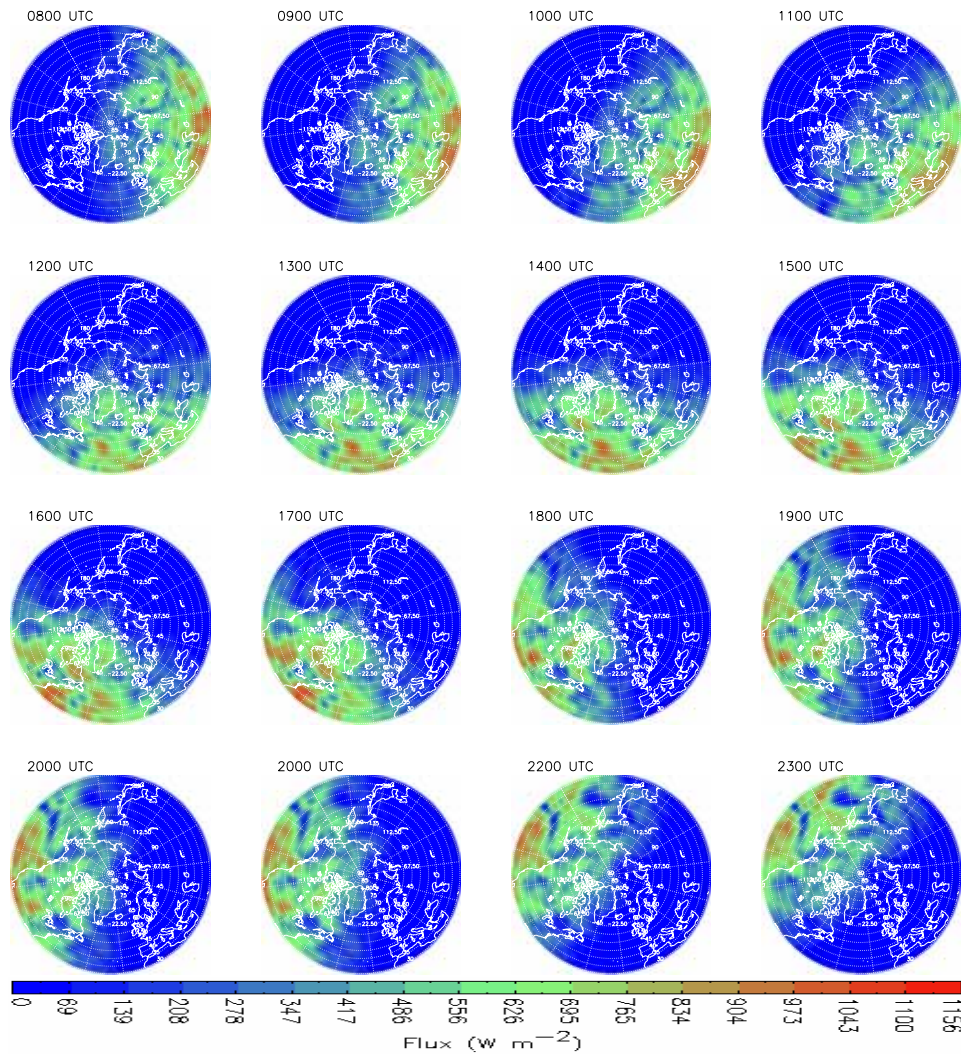
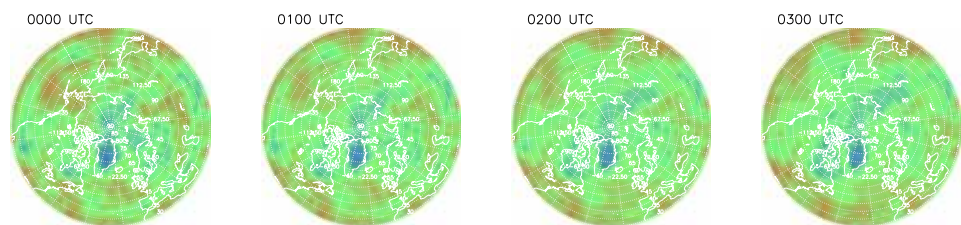


Fig. 8. Hourly snapshots of the downwelling shortwave fluxes at the surface over the Northern Hemisphere region north of 30°N over 24 hours on July 3, 1999. UTC time is labeled at the upper left corner of each hourly snapshot.



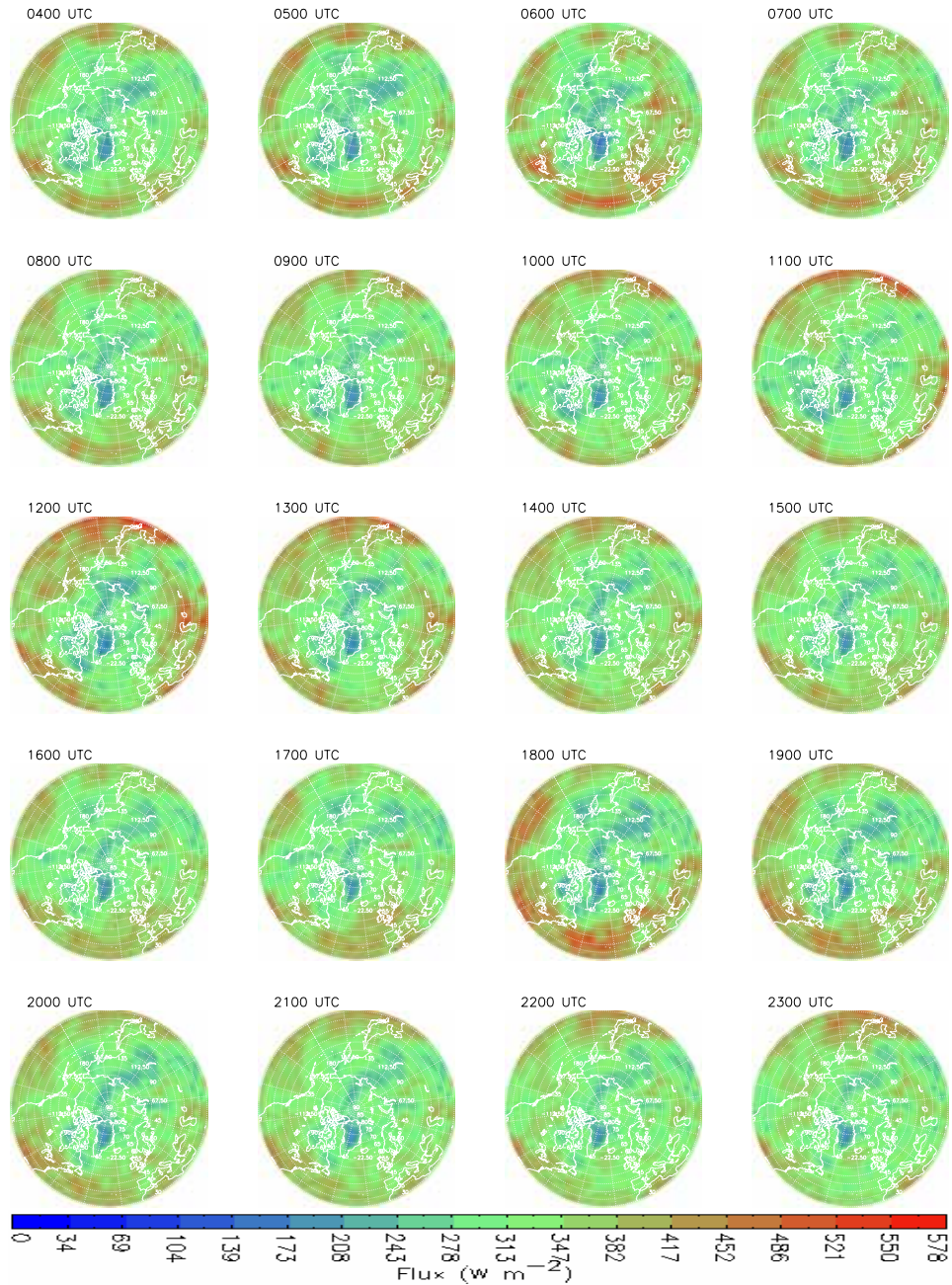
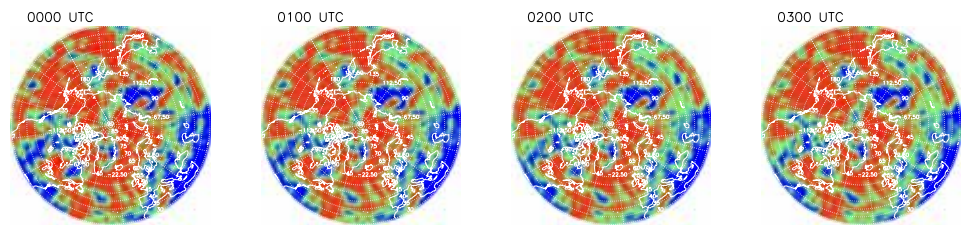


Fig. 9. Same as Figure 8, but for the downwelling longwave fluxes at the surface.



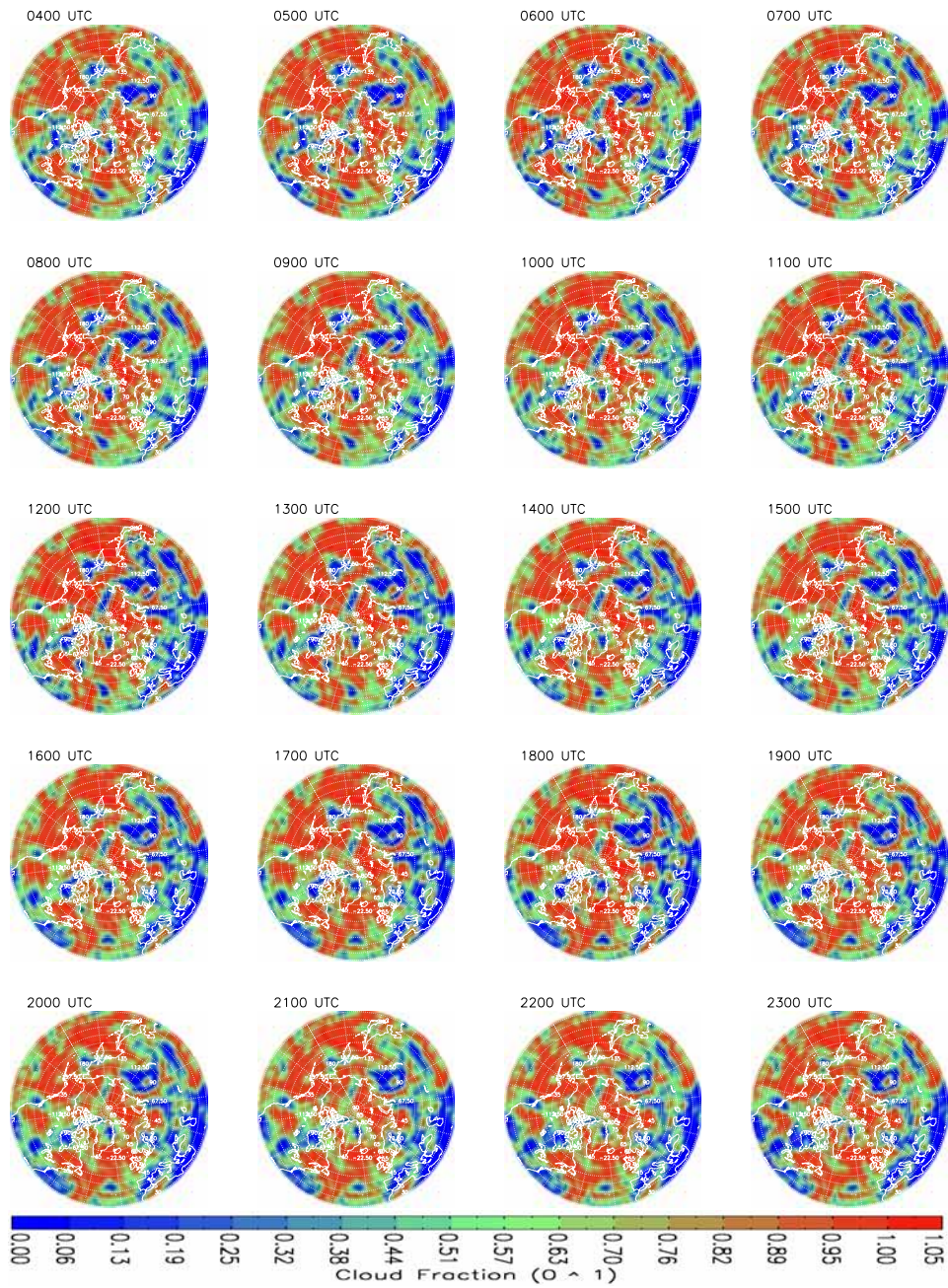


Fig. 10. Same as Figure 8, but for cloudiness.

7. SUMMARY

A diurnal cycle data set of the Arctic surface downwelling shortwave and longwave radiative fluxes at relatively high spatial resolution is needed not only for diurnal cycle studies but also for land surface modeling. Satellite products with relatively high spatial resolution can be

assimilated into global or regional numerical models and blended with model products such as the ERA-40 reanalysis products, as described above, to provide the best possible estimates of climate variables for a better understanding and analysis of Arctic climate change. It has not been previously possible to obtain adequate Arctic descriptions of diurnal variations of surface downwelling shortwave and longwave radiative fluxes because of the lack of ground observations and the limited and/or biased capability of numerical models for the polar region.

This study has developed an approach for deriving diurnal cycles of the surface downwelling shortwave (SSRD) and longwave (STRD) radiative fluxes from a blend of the 6-hourly ERA-40 reanalysis and the APP-x satellite data set, applicable to not only clear-sky conditions but also cloudy-sky conditions. The comparisons of the SSRD and STRD diurnal cycles with respect to the ground-based measurements at Kougarok, Alaska, show that APP-x is better than the ERA-40 for the estimates of SSRD and STRD, indicating the potential to develop algorithms to correct biases resulting in ERA-40 diurnal cycles. Consequently, algorithms have been developed to correct the biases in the ERA-40 data set, and the correction methods are used to derive the ERA-40 diurnal cycle data set. The blending of the APP-x data with the ERA-40 diurnal cycle data proves successful and effective in the creation of reliable and more accurate diurnal cycle data set as verified by the comparisons between the "corrected" and "uncorrected" products with ground-based measurements. The overall standard deviations of SSRD and STRD in the corrected product are reduced to 44.82Wm^{-2} and 31.96Wm^{-2} from 59.51Wm^{-2} and 84.12Wm^{-2} , respectively, in the uncorrected product with respect to the ground-based measurements. The diurnal cycle data set of SSRD, STRD, and cloudiness was derived from the ERA-40 reanalysis products blended with the APP-x products for the North-Hemisphere region north of 30°N over 1982-2000 for further diurnal cycle study.

Future work includes an application of the diurnal cycle data set to study climatological features of surface downwelling shortwave and longwave radiative fluxes, to drive land surface model runs as initial conditions, and to find possible Arctic climate change mechanisms related to the surface radiative fluxes.

Acknowledgments

This work was supported by the National Science Foundation (NSF; Grants OPP-0230317 and OPP-0240827) and the National Oceanic and Atmospheric Administration (NOAA) Arctic Research Office SEARCH program. The National Snow and Ice Data Center (NSIDC) provided the standard APP data set. The NCEP/NCAR reanalysis global profile data set was provided by NOAA-CIRES Climate Diagnostics Center. NASA Langley Research Center provided the ISCCP D2 ozone data set. The European Centre for Medium-Range Weather Forecasts (ECMWF) provided 40-year reanalysis (ERA-40) data. The views, opinions, and findings contained in this report are those of the author(s) and should not be construed as an official National Oceanic and Atmospheric Administration or U.S. Government position, policy, or decision.

References

1. M. M. Holland and C. M. Bitz, "Polar amplification of climate change in coupled models," *Clim. Dyn.* **21**, 221-232 (2003) [doi:10.1007/s00382-003-0332-6].
2. J. E. Walsh, V. M. Kattsov, W. L. Chapman, V. Govorkova and T. Pavlova, "Comparison of Arctic Climate Simulations by Uncoupled and Coupled Global Models," *J. Clim.* **15**, 1429-1446 (2002) [doi:10.1175/1520-0442].
3. J. E. Walsh, S. J. Vavrus and W. L. Chapman, "Workshop on Modeling of the Arctic

- Atmosphere,” *Bull. Am. Meteorol. Soc.* **86**, 845-852 (2005) [doi:10.1175/BAMS-86-6-845].
4. J. E. Walsh and M. S. Timlin, “Northern Hemisphere sea ice simulations by global climate models,” *Polar Res.* **22**, 75-82 (2003).
 5. X. Wang and J. R. Key, “Recent Trends in Arctic Surface, Cloud, and Radiation Properties from Space,” *Science* **299**, 1725-1728 (2003) [doi:10.1126/science.1078065].
 6. X. Wang and J. R. Key, “Arctic Surface, Cloud, and Radiation Properties Based on the AVHRR Polar Pathfinder Dataset. Part I: Spatial and Temporal Characteristics,” *J. Clim.* **18**, 2558-2574 (2005) [doi:10.1175/JCLI3438.1].
 7. X. Wang and J. R. Key, “Arctic Surface, Cloud, and Radiation Properties Based on the AVHRR Polar Pathfinder Dataset. Part II: Recent Trends,” *J. Clim.* **18**, 2575-2593 (2005) [doi:10.1175/JCLI3439.1].
 8. J. A. Francis, E. Hunter, J. R. Key and X. J. Wang, “Clues to variability in Arctic minimum sea ice extent,” *Geophys. Res. Lett.* **32**, L21501 (2005) [doi:10.1029/2005GL024376].
 9. M. C. Serreze, J. E. Walsh, F. S. Chapin III, T. Osterkamp, M. Dyurgerov, V. Romanovsky, W. C. Oechel, J. Morison, T. Zhang and R. G. Barry, “Observational Evidence of Recent Change in the Northern High-Latitude Environment,” *Clim. Change* **46**, 159-207 (2000) [doi:10.1023/A:1005504031923].
 10. M. C. Serreze, M. P. Clark and D. H. Bromwich, “Monitoring Precipitation over the Arctic Terrestrial Drainage System: Data Requirements, Shortcomings, and Applications of Atmospheric Reanalysis,” *J. Hydrometeorol.* **4**, 387-407 (2003) [doi:10.1175/1525-7541(2003)4<387:MPOTAT>2.0.CO;2].
 11. M. C. Serreze, J. A. Maslanik, T. A. Scambos, F. Fetterer, J. Stroeve, K. Knowles, C. Fowler, S. Drobot, R. G. Barry and T. M. Haran, “A record minimum arctic sea ice extent and area in 2002,” *Geophys. Res. Lett.* **30**, 1110 (2003) [doi:10.1029/2002GL016406].
 12. J. E. Walsh and W. L. Chapman, “20th-Century Sea-Ice Variations from Observational Data,” *Ann. Glaciol.* **33**, 444-448 (2001).
 13. J. A. Maslanik, M. C. Serreze and T. Agnew, “On the record reduction in 1998 western Arctic sea-ice cover,” *J. Geophys. Res.* **26**, 1905-1908 (1999).
 14. A. J. Schweiger, “Changes in seasonal cloud cover over the Arctic seas from satellite and surface observations,” *Geophys. Res. Lett.* **31**, L12207 (2004) [doi:10.1029/2004GL020067].
 15. R. Curry and C. Mauritzen, “Dilution of the Northern North Atlantic Ocean in Recent Decades,” *Science* **308**, 1772-1774 (2005) [doi:10.1126/science.1109477].
 16. J. Liu, J. A. Curry and Y. Hu, “Recent Arctic Sea Ice Variability: Connections to the Arctic Oscillation and the ENSO,” *Geophys. Res. Lett.* **31**, L09211 (2004) [doi:10.1029/2004GL019858].
 17. J. Liu, J. A. Curry, W. B. Rossow, J. R. Key and X. Wang, “Comparison of surface radiative flux data sets over the Arctic Ocean,” *J. Geophys. Res.* **110**, C02015 (2005) [doi:10.1029/2004JC002381].
 18. T. Uttal, J. A. Curry, M. G. McPhee, D. K. Perovich, R. E. Moritz, J. A. Maslanik, P. S. Guest, H. L. Stern, J. A. Moore, R. Turenne, A. Heiberg, M. C. Serreze, D. P. Wylie and O. G. Persson, “Surface Heat Budget of the Arctic Ocean,” *Bull. Am. Meteorol. Soc.* **83**, 255-275 (2002) [doi:10.1175/1520-0477(2002)083<0255:SHBOTA>2.3.CO;2].
 19. S. M. Uppala, P. W. Kallberg, A. J. Simmons, U. Andrae, V. D. Bechtold, M. Fiorino, J. K. Gibson, J. Haseler, A. Hernandez, G. A. Kelly, X. Li, K. Onogi, S. Saarinen, N. Sokka, R. P. Allan, E. Andersson, K. Arpe, M. A. Balmaseda, A. C. M. Beljaars, L. Van De Berg, J. Bidlot, N. Bormann, S. Caires, F. Chevallier, A. Dethof,

- M. Dragosavac, M. Fisher, M. Fuentes, S. Hagemann, E. Holm, B. J. Hoskins, L. Isaksen, P. A. E. M. Janssen, R. Jenne, A. P. McNally, J. F. Mahfouf, J. J. Morcrette, N. A. Rayner, R. W. Saunders, P. Simon, A. Sterl, K. E. Trenberth, A. Untch, D. Vasiljevic, P. Viterbo and J. Woollen, "The ERA-40 reanalysis," *Q. J. R. Meteorol. Soc.* **131**, 2961-3012 (2005) [doi:10.1256/qj.04.176].
20. J. R. Key, *The cloud and surface parameter retrieval (CASPR) system for polar AVHRR*, J. R. Key, Ed., pp. 1-59, Cooperative Institute for Meteorological Satellite Studies, University of Wisconsin, Madison, available online at <http://stratus.ssec.wisc.edu/caspr/documentation.html> (2002).
 21. J. R. Key, X. Wang, J. C. Stoeve and C. Fowler, "Estimating the cloudy-sky albedo of sea ice and snow from space," *J. Geophys. Res.* **106**, 12,489-12,497 (2001) [doi:10.1029/2001JD900069].
 22. J. R. Key and A.J. Schweiger, "Tools for atmospheric radiative transfer: Streamer and FluxNet," *Computers and Geosciences* **24**, 443-451 (1998) [doi:10.1016/S0098-3004(97)00130-1].
 23. J. R. Key, *Streamer User's Guide*, J. R. Key, Ed., pp. 1-107, Cooperative Institute for Meteorological Satellite Studies, University of Wisconsin, Madison, available online at <http://stratus.ssec.wisc.edu/streamer/documentation.html> (2002).
 24. W. B. Rossow, A. Walker, D. Beuschel, and M. Roiter, *International Satellite Cloud Climatology Project (ISCCP) Documentation of Cloud Data*, W. B. Rossow et al, Ed., pp. 1-115, World Climate Research Programme, NASA, Goddard Institute of Space Studies (1996).
 25. J. A. Maslanik, J. Key, C. W. Fowler, T. Nguyen and X. Wang, "Spatial and temporal variability of satellite-derived cloud and surface characteristics during FIRE-ACE," *J. Geophys. Res.* **106**, 15,233-15,249 (2001) [doi:10.1029/2000JD900284].
 26. J. Stroeve, J. Box, C. Fowler, T. Haran, and J.R. Key, "Intercomparison Between in situ and AVHRR Polar Pathfinder-derived Surface Albedo over Greenland," *Remote Sensing of the Environment* **75**, 360-374 (2001) [doi:10.1016/S0034-4257(00)00179-6].
 27. M. J. Pavolonis and J. R. Key, "Antarctic Cloud Radiative Forcing at the Surface Estimated from the AVHRR Polar Pathfinder and ISCCP D1 Datasets, 1985-93," *J. Appl. Meteorol.* **42**, 827-840 (2003) [doi:10.1175/1520-0450(2003)042<0827:ACRFAT>2.0.CO;2].
 28. J. R. Key, R. A. Silcox and R. S. Stone, "Evaluation of surface radiative flux parameterizations for use in sea ice models," *J. Geophys. Res.* **101**, 3839-3849 (1996) [doi:10.1029/95JC03600].
 29. T. J. Bennett, "A Coupled Atmosphere-Sea Ice Model Study of the Role of Sea Ice in Climatic Predictability," *J. Atmos. Sci.* **39**, 1456-1465 (1982) [doi:10.1175/1520-0469(1982)039<1456:ACASIM>2.0.CO;2].
 30. J. D. Jacobs, "Radiation climate of Broughton Island, Energy budget studies in relation to fast-ice breakup processes in Davis Strait," *Occas. Pap.* **26**, 105-120 (1978).
 31. S. B. Idso and R. D. Jackson (1969), "Thermal radiation from the atmosphere," *J. Geophys. Res.* **74**, 5379-5403 (1969).
 32. L. D. Hinzman, N. D. Bettez, W. R. Bolton, F. S. Chapin, M. B. Dyurgerov, C. L. Fastie, B. Griffith, R. D. Hollister, A. Hope, H. P. Huntington, A. M. Jensen, G. J. Jia, T. Jorgenson, D. L. Kane, D. R. Klein, G. Kofinas, A. H. Lynch, A. H. Lloyd, A. D. McGuire, F. E. Nelson, W. C. Oechel, T. E. Osterkamp, C. H. Racine, V. E. Romanovsky, R. S. Stone, D. A. Stow, M. Sturm, C. E. Tweedie, G. L. Vourlitis, M. D. Walker, D. A. Walker, P. J. Webber, J. M. Welker, K. Winker and K. Yoshikawa, "Evidence and implications of recent climate change in northern Alaska and other

- arctic regions,” *Clim. Change* **72**, 251-298 (2005) [doi:10.1007/s10584-005-5352-2].
33. M. Jin and R. E. Dickinson, “Interpolation of surface radiative temperature measured from polar orbiting satellites to a diurnal cycle. Part 1: Without clouds,” *J. Geophys. Res.* **104**, 2105-2116 (1999) [doi:10.1029/1998JD200005].
 34. M. Jin, “Interpolation of surface radiative temperature measured from polar orbiting satellites to a diurnal cycle. Part 2: Cloudy-pixel treatment,” *J. Geophys. Res.* **105**, 4061-4076 (2000) [doi:10.1029/1999JD901088].

Xuanji Wang is an assistant researcher at the Space Science and Engineering Center of the University of Wisconsin-Madison. He received his PhD degree in Atmospheric and Oceanic Sciences from the University of Wisconsin-Madison in 2003. His current research interests include hyperspectral radiation transfer, remote sensing of cloud, surface, radiation, and atmospheric properties, and satellite meteorology and climatology of the polar regions.

Jeffrey R. Key is the Branch Chief of the Advanced Satellite Products Branch, Center for Satellite Applications and Research (STAR), NOAA/NESDIS. He received his PhD degree from the University of Colorado-Boulder in 1988. Dr. Key's research is in satellite meteorology and climatology of the polar regions. Current research topics include the spatial and temporal variability of polar cloud, surface, and radiation properties, polar winds, and recent climate trends.

Chuck Fowler: biography not available.

James Maslanik: James A. Maslanik received the Ph.D. degree in geography from the University of Colorado, Boulder in 1984 and Masters of Environmental Pollution Control and Bachelor of Science in Forest Science from the Pennsylvania State University in 1980 and 1978 respectively. He is a research professor in the Department of Aerospace Engineering Sciences at the University of Colorado, Boulder. His research interests include the interactions of sea ice with atmosphere and ocean, remote sensing and field investigations of sea ice properties, effects of climate change on Arctic coastal communities, and development and deployment of unpiloted aerial vehicles for polar research.